

Small Intestinal Submucosa: A Tissue-Derived Extracellular Matrix That Promotes Tissue-Specific Growth and Differentiation of Cells *in Vitro*

SHERRY L. VOYTIK-HARBIN, M.S.E.E., Ph.D.,¹ ANDREW O. BRIGHTMAN, Ph.D.,¹
BEVERLY Z. WAISNER, B.S.,² J. PAUL ROBINSON, Ph.D.,² and
CARLTON H. LAMAR, D.V.M., Ph.D.²

ABSTRACT

The importance of understanding cell-extracellular matrix (ECM) interaction is now evident as scientists, engineers, and physicians search for novel scaffolds that support and maintain tissue-specific cellular growth and function both *in vivo* and *in vitro*. Small intestinal submucosa (SIS) represents an ECM that has been derived from porcine intestine while preserving its natural composition and architecture. More recently, an extract of this physiologic ECM, which forms a three-dimensional gel *in vitro*, has been developed. When compared to routinely used culture substrata (e.g., plastic, Vitrogen, and Matrigel), intact SIS and SIS-derived gel possess unique compositional and architectural features. Simple squamous epithelial (pulmonary artery), fibroblastic (Swiss 3T3), glandular epithelial (adenocarcinoma), and smooth muscle-like (urinary bladder) cells were seeded upon intact SIS and SIS-derived gel and their morphologic response evaluated. For each of the four cell types studied, intact SIS and SIS-derived gel were equivalent or superior in their ability to support and maintain expression of tissue-specific phenotype when compared to the routinely used substrata, plastic, Vitrogen, and Matrigel. Therefore, SIS may provide a novel biologically derived scaffold for the growth and study of a variety of cell types *in vitro*. Such information regarding the influence of substrate structure and function on cell behavior will be useful in the development of successful tissue engineering strategies.

INTRODUCTION

INTERACTION OF CELLS WITH THEIR EXTRACELLULAR MATRIX (ECM) plays a crucial role in the organization, homeostasis, and function of all tissues and organs. It is the continuous cross-talk between cells and the surrounding matrix environment that orchestrates critical processes such as the acquisition and maintenance of differentiated phenotypes during embryogenesis, the development of form (morphogenesis), angiogene-

¹Hillenbrand Biomedical Engineering Center and ²Department of Basic Medical Science, School of Veterinary Medicine, Purdue University, West Lafayette, Indiana 47907.

This work was presented in part at the Inaugural Meeting of the Tissue Engineering Society, held in Orlando, Florida, December 13-15, 1996.

sis, wound healing, and even tumor metastasis. The cell and its ECM are said to exist in a state of "dynamic reciprocity".^{1,2} Both biochemical and biophysical signals from the ECM modulate fundamental cellular activities, including adhesion, migration, proliferation, differential gene expression, and programmed cell death.^{3,4} In turn, the cell can modify its ECM environment by modulating synthesis and degradation of specific matrix components. The realization of the significance of cell-ECM communication has led to a renewed interest in characterizing ECM constituents and the basic mechanisms of cell-ECM interaction.

To provide an *in vitro* culture environment that would more closely mimic cell-ECM interaction *in vivo*, purified ECM components such as collagen, fibronectin, laminin, and glycosaminoglycans (e.g., hyaluronic acid, heparin sulfate) have been used to derivatize artificial substrata for augmentation of cell adhesion, growth, and morphology. Three-dimensional culture matrices also have been fashioned from purified ECM components, specifically fibrin clots⁵ and collagen gels.⁶ Investigations with these matrices have demonstrated the importance of three-dimensional architecture in the establishment of a tissue-like histology.

More complex scaffolds representing combinations of ECM components in a natural or processed form have also been studied. These include reconstituted basement membrane extract from Engelbreth Holm Swarm tumor (Matrigel), and allogeneic and xenogeneic tissues (including lens capsule,⁷ liver,⁸ amnion,⁹ and chorioallantoic membrane¹⁰). Although these substrata allow the study of cell growth and differentiation in a more physiologically relevant system, their use has been limited by availability and amenability to disinfection, sterilization, and manufacturing processes.

Previous *in vivo* studies have shown that SIS modulates the cellular activities of the remodeling and repair responses when implanted in a number of different tissue microenvironments, including lower urinary tract,^{11,12} body wall,¹³ tendon,¹⁴ ligament,¹⁵ bone (Voytik-Harbin, unpublished data), and blood vessels.¹⁶ Compositional analyses of the material have shown that, like other normal connective tissues, the material consists predominantly of fibrillar collagens (types I, III, V; unpublished data), with lesser quantities of proteoglycans, glycosaminoglycans (e.g., hyaluronic acid),¹⁷ glycoproteins (e.g., fibronectin),¹⁸ and growth factors (e.g., FGF-2 and TGF β -related protein).¹⁹ It appears likely that SIS, because of its complex composition and architecture, could be useful for *in vitro* cell culture, where maintenance of differentiated phenotype is important.

In this communication, we report on the ability of SIS to support the survival and growth of several different cell types, including fibroblasts (Swiss mouse 3T3), simple squamous epithelium (rat pulmonary artery endothelium), glandular epithelium (canine prostate adenocarcinoma), and smooth muscle-like cells (human urinary bladder). The morphologic response of these cell types to intact SIS, SIS-derived gel, and other widely used substrata (plastic, Matrigel, and Vitrogen) was evaluated and compared. In addition, the structural and compositional features of the substrata were compared.

MATERIALS AND METHODS

Cell Culture

Swiss mouse 3T3 fibroblasts were obtained from American Type Culture Collection (ATCC) (Rockville, MD). Primary human urinary bladder stromal cells (HUBS) were derived from bladders of patients undergoing ureteral reimplantation for vesicoureteral reflux and generously provided by Dr. E. Cheng, Northwestern University (Chicago, IL). Primary canine prostate carcinoma cells were established from a primary tumor of a dog with prostate adenocarcinoma and were kindly provided by Dr. D. Waters, Purdue University (West Lafayette, IN). Rat pulmonary endothelial cells were isolated from rat pulmonary arteries, purified by flow cytometric fluorescence-activated cell sorting.²⁰ The cell types, source information, and medium conditions involved in these experiments are summarized in Table 1.

Substrata

Vitrogen and Matrigel were obtained from Collagen Corporation (Fremont, CA) and Collaborative Biomedical (Bedford, MA), respectively. All tissue culture plastics were obtained from Corning Inc. (Corning, NY).

SMALL INTESTINAL SUBMUCOSA

TABLE 1. SUMMARY OF CELL TYPES AND NUTRIENTS

Name	Origin/Source	Medium
3T3	Swiss mouse embryo fibroblasts; American Type Culture Collection, CRL 1658	DMEM (Dulbecco's modified Eagle's medium) with 1.5 g/L NaHCO ₃ , 10% NNCS (neonatal calf serum), 100 U/ml penicillin, 100 µg/ml streptomycin, 2 mM L-glutamine
RPEC	Rat pulmonary artery endothelial cells; J. P. Robinson, Purdue University	RPMI 1640, 5% NCS (newborn calf serum), 5% FBS (fetal bovine serum), 100 U/ml penicillin, 100 µg/ml streptomycin, 2 mM L-glutamine
HUBS	Human urinary bladder stromal cells; E. Cheng, Northwestern University	Modified medium 199 supplemented with 10% NCS (newborn calf serum), 2.5 µg/ml fungizone and 50 µg/ml gentamicin (Baskin et al., 1993); medium modifications included the addition of sodium bicarbonate (2.2 g/L), bactopectone (0.5 g/L), glucose (3.0 g/L), L-glutamine (0.29 g/L), HEPES (3.57 g/L), 100× BME vitamins (10 ml/L, Flow Labs), and 100× BME amino acids (10 ml/L, Gibco, Grand Island, New York)
Clemons	Canine prostate adenocarcinoma; D. Waters, Purdue University	RPMI 1640, 10% FBS, 100 U/ml penicillin, 100 µg/ml streptomycin, 2 mM L-glutamine

Preparation of intact SIS and SIS-derived gel. Intestinal submucosa was prepared from the small intestines of market weight pigs obtained from a local meat processing plant. In brief, intestine was rinsed free of contents and everted, and the superficial layers of the mucosa were removed by mechanical delamination. The tissue was reverted to its original orientation and the external muscle layer removed. The prepared intestinal submucosa tube was split open longitudinally and rinsed extensively in water to lyse any cells associated with the matrix and to eliminate cell degradation products. Immediately after rinsing, intestinal submucosa was disinfected with 0.1% peracetic acid for cell culture or frozen in liquid nitrogen and stored at -80°C for preparation of SIS-derived gel.

For preparation of SIS-derived gel, frozen tissue first was pulverized under liquid nitrogen with an industrial blender and stored at -80°C prior to use. SIS powder (5% w/v) was suspended in 0.5 M acetic acid containing 0.1% pepsin and vigorously stirred for 72 h at 4°C . The mixture then was centrifuged at 12,000 rpm for 20 min at 4°C to remove undigested tissue. The supernatant was dialyzed extensively against 0.01 M acetic acid at 4°C in spectrapor tubing (MWCO 3500, Spectrum Medical Industries). To obtain a sterile preparation, the solution was dialyzed against 0.01 M acetic acid containing chloroform (approximately 0.5% v/v), followed by several changes of sterile 0.01 M acetic acid. To polymerize the SIS extract, 1.2 ml 10× PBS (1.37 M NaCl, 26.8 mM KCl, 0.1 M Na₂HPO₄, and 17.6 mM KH₂PO₄, and 5 mg/L phenol red, pH 7.4) and 1.2 ml 0.1 NaOH were added to 8 ml of SIS extract. This solution was brought to pH 7 with 0.1 M HCl, aliquotted into 24-well plates, and gelled at 37°C for 30–60 min.

Scanning Electron Microscopy

Substrata were fixed in 3% glutaraldehyde in Millonig's buffer and post fixed in 1% osmium tetroxide. Fixed specimens were dehydrated in a graded series of acetones, critical point dried, affixed to scanning stubs, and sputter coated with gold/palladium. Specimens were viewed with a JEOL JSM-840 scanning electron microscope. Gelled substrata also were quick frozen by plunging into a liquid nitrogen slush without prior fixation or dehydration. The sample was transferred into a CT1000 coldstage attachment (Oxford Instruments North America, Inc., Concord, MA), and the surface was fractured and coated with gold prior to viewing at temperatures of -150°C with the SEM.

Cell Growth on Substrata

Twenty-four-well tissue culture plates were prepared with Matrigel (500 μl /well), Vitrogen (500 μl /well), SIS, SIS-derived gel (500 μl /well), or no substrate. SIS material was affixed in polypropylene frames, with the mucosal surface facing upward to create a well area of 0.5 cm^2 . All substrata were equilibrated with sterile PBS, pH 7.4, prior to the application of cells.

Cells were harvested in complete medium (Table 1) and seeded upon substrata at 60,000 cells/ cm^2 . For certain experiments, cells were labeled with the fluorescent cell membrane dye PKH26 (Sigma, St. Louis, MO) prior to seeding upon the substrata. Culture plates were incubated at 37°C in a humidified atmosphere of 5% CO_2 in air and fed two to three times weekly. On days 1, 4, 7, and 14, the cells and associated substrate (intact SIS only) were fixed and processed for light or fluorescence microscopy.

Fluorescence microscopy. Cells labeled with fluorescent markers were fixed in 4% paraformaldehyde and observed using a fluorescence microscope (Labophot, Nikon).

Light microscopy. Cell growth on plastic, Matrigel, Vitrogen, and SIS-derived gel was observed daily using a standard inverted microscope. Digital images were collected on days 1, 4, 7, 11, and 14 using an inverted microscope, video camera (Sanyo, Japan), and Digital Video Producer software (Asymetrix) on a 755CD laptop computer (IBM).

Histology. Cells and associated substrata were fixed in neutral buffered formalin, embedded in paraffin, sectioned to 6 μm , and stained with H&E. Morphological evaluation was conducted using light microscopy.

RESULTS

Morphological Appearance and Characterization

It has been well documented that physical, geometrical, and topological features of substrata affect cell behavior both *in vitro* and *in vivo*.²¹ Therefore, architectural features of SIS, SIS-derived gel, Vitrogen, and Matrigel were determined and subsequently compared. Small intestine represents a multilayered organ consisting of mucosa, lamina propria, muscularis mucosa, submucosa, muscularis externa, and serosa (Fig. 1). Preparation of SIS involved mechanical removal of the outermost epithelial and muscle layers. Treatment of the remaining submucosa, muscularis mucosa, and remnant lamina propria layers under hypotonic conditions provided an acellular ECM designated SIS. Initial structural analysis was performed using routine critical point drying of specimens followed by scanning electron microscopy (SEM). Low-magnification SEM demonstrated the disparity in the topography of the mucosal and serosal surfaces of SIS (Fig. 2). The relatively smooth mucosal surface, which once supported the epithelial lining of the intestine, showed multiple folds and involutions (Fig. 2A), whereas the fibrillar nature of the serosal side was evidenced by its more ragged appearance (Fig. 2C). Ultrastructurally, the mucosal surface was characterized by more densely packed fibers, which form discontinuous layers varying in orientation (Fig. 2B). Alternatively, the serosal side exhibited a fine network of loosely organized fibers, most of which are <1 μm in diameter (Fig. 2D). Although most fibers appeared to be organized randomly, some formed assemblies to create larger fibers. Analysis of SIS-derived gel (Fig. 3A) and Vitrogen (Fig. 3C) prepared using critical point drying techniques demonstrated a tightly woven network of small-diameter fibrils with extensive lateral association. Matrigel, on the other hand, featured a more densely compact, sheet-like surface (Fig. 3E). Although some appreciation of substrate architecture was obtained from critical point dried specimens, excessive shrinkage was noted. To minimize the possibility of structural artifacts induced by such preparatory techniques, quick-freeze, cold-stage SEM was employed. This technique obviated the need for both chemical fixation and dehydration. Results obtained using this method more accurately represent the detailed macromolecular structure of samples with high water content. With cold-stage SEM, the marked differences in the ultrastructure of the three substrata were obvious. SIS-derived gel consisted of a network of loosely organized fibrils that varied in size (Fig. 3B). The fine fibers composing Vitrogen appeared more randomly oriented and formed regions of dense aggregates with extensive cross-branching (Fig. 3D). Matrigel featured a honeycomb lattice with very fine, cobweb-like fibers decorating the individual honeycomb cells (Fig. 3F).

SMALL INTESTINAL SUBMUCOSA

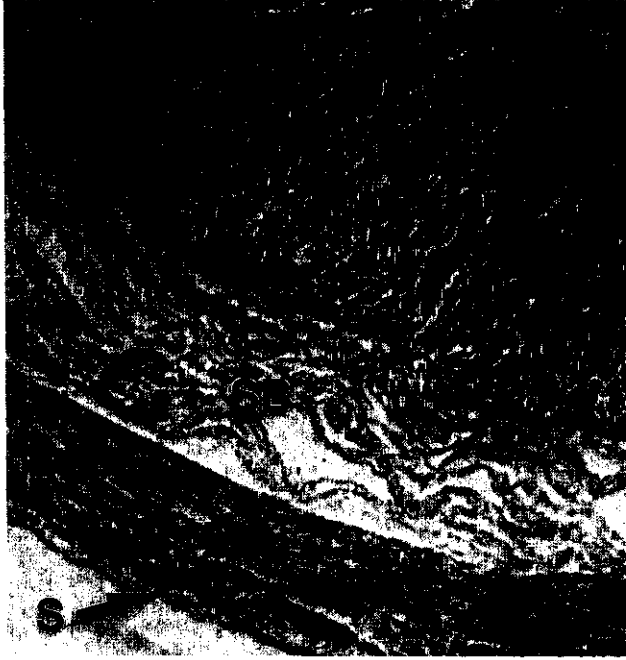


FIG. 1. Light micrograph of H&E-stained cross-section of porcine small intestine. Note the layered structure E = epithelial layer; MM = muscularis mucosa; SB = submucosa; ME = muscularis externa; S = serosa. SIS represents the submucosal layer with adjacent muscularis mucosa and remnant lamina propria (not visible at this magnification). Bar = 100 μ m.

Effect of Substratum on Cellular Behavior and Morphology

The SIS matrix provided a ready source of ECM, and its mucosal surface supported distinct morphological responses of the four different cell types studied—fibroblasts (Swiss mouse 3T3), endothelium (rat pulmonary artery), glandular epithelium (canine prostate adenocarcinoma), and smooth muscle-like cells (human urinary bladder stromal). In all cases, specific cell-SIS interactions more closely approximated those observed *in vivo*, especially when compared to plastic, Matrigel, and Vitrogen (Table 2).

Fibroblasts. Swiss 3T3 fibroblasts, when grown on plastic, readily proliferated and exhibited a spindle-shaped morphology at subconfluence (Fig. 4A). At confluence, achieved within 4 days, these cells demonstrated contact inhibition and appeared more cuboidal in shape. Fibroblasts responded in a similar fashion to the three-dimensional collagen gel, Vitrogen (Fig. 4B). After 4 days, the cells had formed a confluent monolayer of cuboidal shaped cells along the substrate surface. The presence of a few spindly, elongated shaped cells in focal planes below the surface suggested penetration of a limited number of individual cells into the collagen matrix. The same cells showed a dramatically different response when grown on Matrigel. Within 24 h, fibroblasts appeared spindle-shaped but formed regional aggregates (Fig. 4C). These aggregates persisted throughout the 14-day timecourse with no obvious proliferative activity. When applied to SIS-derived gel, fibroblasts maintained a spindly, elongated shape throughout the 14-day observation period. The ability of fibroblasts to proliferate and more readily penetrate the SIS-derived gel was evidenced by numerous fibroblasts in multiple focal planes along and within the matrix (Fig. 4D). Intimate cell-cell contact was not apparent; however, the cells within a single focal plane did show parallel alignment. The invasion and morphological characteristics of fibroblasts on SIS-derived gel resembled those observed *in vivo*. Similar *in vivo*-like behavior was observed by fibroblasts seeded on the mucosal side of intact SIS. The cells were fusiform to spindly in shape, and actively proliferated and migrated into the tortuous fiber network of the small intestinal matrix (Fig. 5). The fibroblasts appeared as individual cells compressed

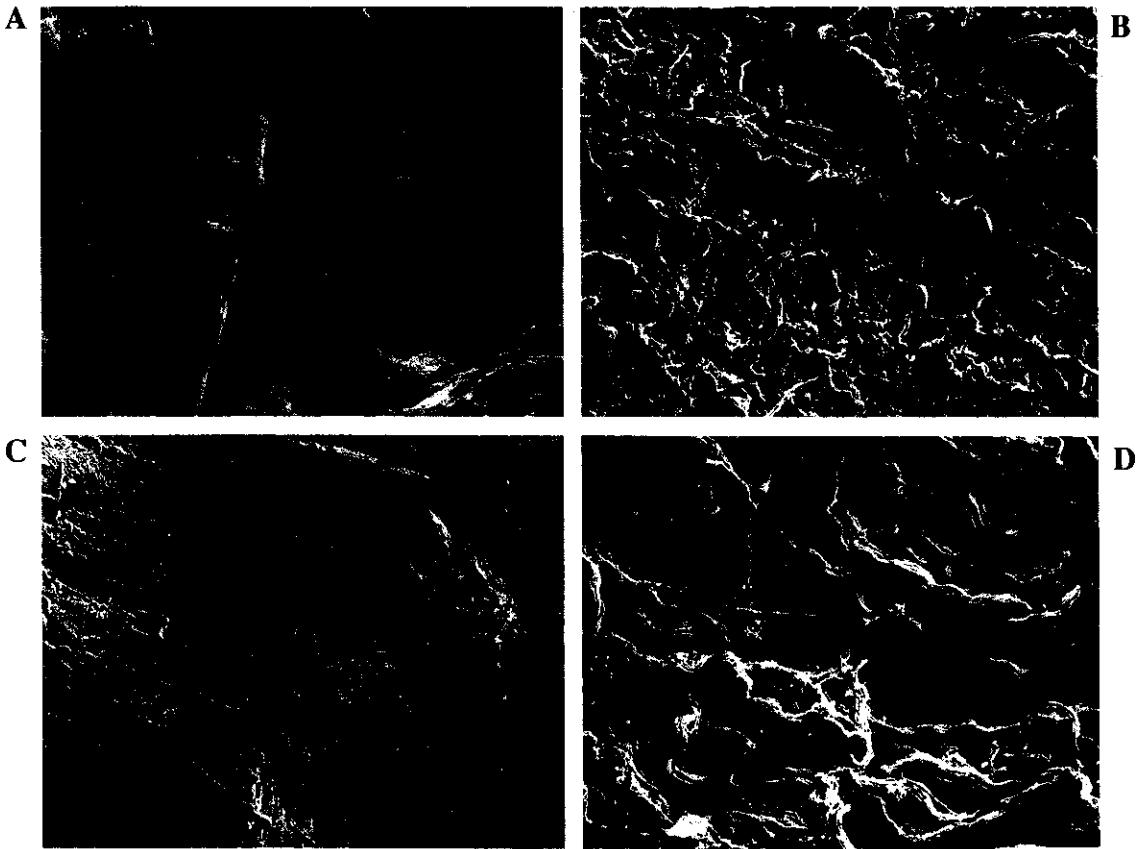


FIG. 2. Scanning electron micrographs of mucosal ($\times 50$, A; $\times 1,000$, B) and serosal ($\times 50$, C; $\times 1,000$, D) surfaces of intact SIS. The fiber network of the mucosal surface forms a densely packed sheet-like surface, whereas the fibers of the serosal surface are randomly arranged in a loose network. Bars = 100 and 10 μm for $\times 50$ and $\times 1,000$ magnifications, respectively.

among the collagenous fibers, suggesting active cell–ECM as well as cell–cell interaction. Taken together, the three-dimensional growth pattern and behavior of fibroblasts on SIS as well as the natural ECM architecture inherent to SIS were reminiscent of connective tissue *in vivo*.

Endothelium. A homogeneous population of endothelial cells was derived from rat pulmonary arteries, followed by fluorescence-activated cell sorting using flow cytometry.²⁰ On plastic, these cells displayed the traditional “cobblestone” morphology, characteristic of most macrovascular endothelial cells (Fig. 6A). A different morphological pattern was exhibited by these endothelial cells when grown on Vitrogen (Fig. 6B) and SIS-derived gel (Fig. 6D). On both substrata, endothelial cells appeared spindle- to stellate-shaped with multiple cytoplasmic projections. By day 7, the cells proliferated to form confluent monolayers of spindly to round shaped cells. Little to no penetration of cells into either Vitrogen or SIS-derived gel was observed. As with fibroblasts, endothelial cells showed a distinct response to Matrigel (Fig. 6C). A rapid aggregation of cells was observed within 24 h. Interestingly, some aggregates were connected by long canalicular-like processes, which regressed by 72 h. Although endothelial cells readily and rapidly proliferated on plastic, Vitrogen, and SIS-derived gel, no significant increase in cell number was observed on Matrigel. On SIS, rat pulmonary endothelial cells grew primarily along the surface of the substrate as cuboidal shaped cells creating a “cobblestone” pattern (Fig. 7A). At early time points, cell–cell interaction predominated such that the cells formed a cellular layer one to two cells thick, reminiscent of the endothelial layer common to blood vessels (Fig. 7B). At later time points, endothelial cells were seen to penetrate the matrix and in some cases formed a new endothelial lining along preexisting vessel tunnels.

SMALL INTESTINAL SUBMUCOSA

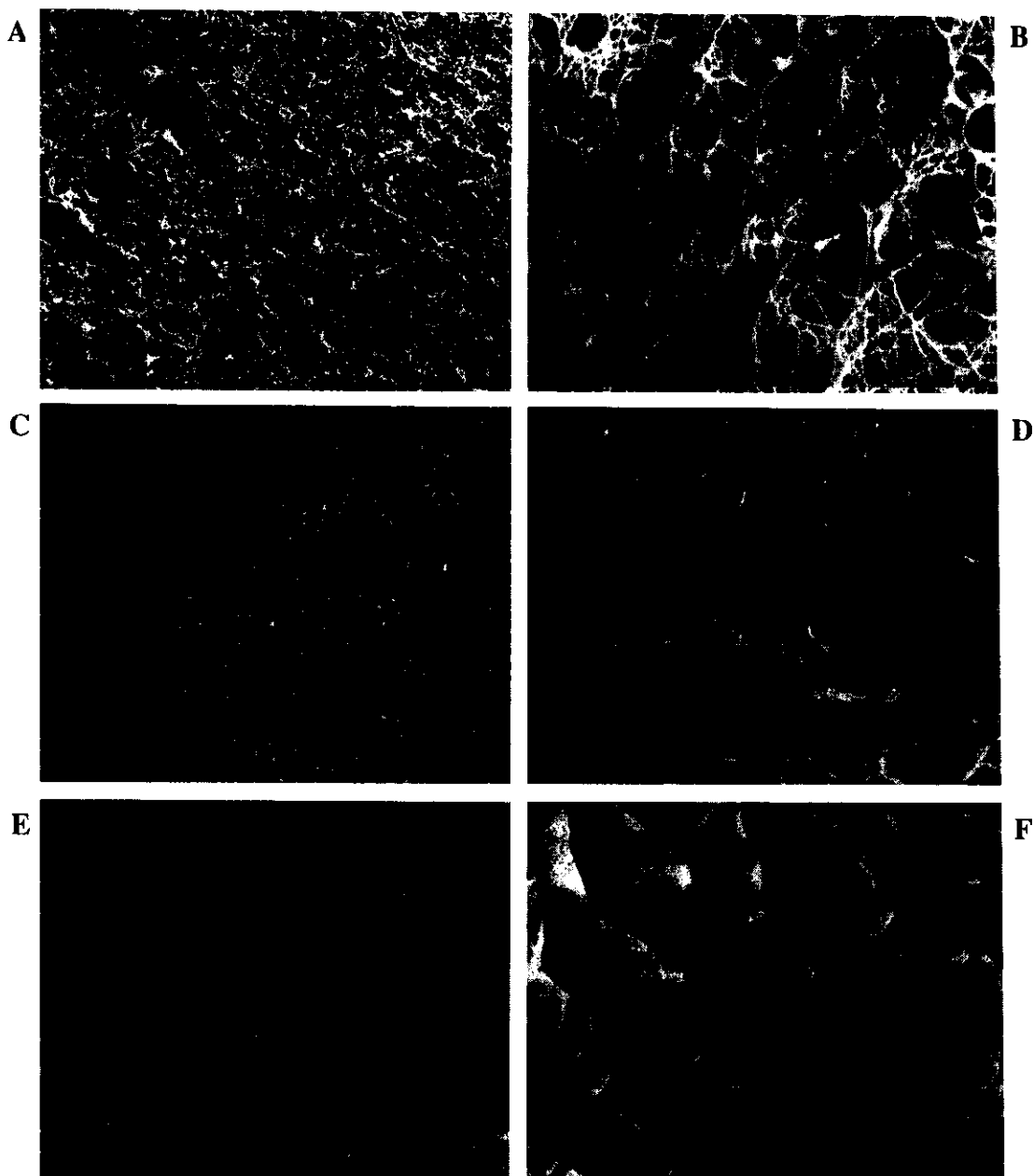


FIG. 3. Scanning electron micrographs ($\times 1,000$) demonstrating the ultrastructure of SIS-derived gel, Vitrogen, and Matrigel. (A,C,E) Specimens prepared using critical point drying. (B,D,F) Cold stage preparation of gelled samples. Bar = 10 μm .

Glandular Epithelium

The canine prostate carcinoma cell line, Clemons, used in this study was originally isolated from a primary tumor and propagated in culture. Immunohistochemical staining confirmed the presence of cytokeratin, an intracellular marker characteristic of the epithelial cell phenotype. During the first 24 h of culture, Clemons cells attached and appeared morphologically similar on plastic, Vitrogen, and SIS-derived gel. On all three substrata, the cells grew initially as flattened cells, most of which coalesced to form heterogeneous shaped patterns. After 4 days in culture, subtle differences were observed in the cellular response to SIS-derived gel compared to the other two substrata. On Vitrogen and plastic, the cells continued to grow along

TABLE 2. EFFECT OF SUBSTRATA ON BEHAVIOR AND MORPHOLOGY OF DIFFERENT CELL TYPES

Cell type	Substrate				
	Plastic	Vitrogen	Matrigel	SIS-derived gel	Intact SIS
Fibroblasts					
Shape	Spindle; cuboidal upon confluence	Spindle; cuboidal upon confluence	Spindle to round	Spindle	Spindle
Prolif	Yes; contact inhibition	Yes; contact inhibition	Limited to none	Yes	Yes
Morph	Two-dimensional monolayer	Two-dimensional monolayer; limited matrix penetration	Rapid aggregate formation	Three-dimensional; spindle-shaped cells along surface of and within matrix	Three-dimensional; spindle-shaped cells along surface of and within matrix
Endothelium					
Shape	Cobblestone	Spindle to stellate	Variable	Spindle to stellate	Cobblestone
Prolif	Yes	Yes	Limited to none	Yes	Yes
Morph	Two-dimensional monolayer	Three-dimensional multilayers (1-3 cells thick); limited matrix penetration	Rapid aggregate formation; canalicular-like processes	Three-dimensional multilayers (1-3 cells thick); limited matrix penetration	Three-dimensional multilayers (1-3 cells thick); matrix penetration
Glandular epithelium					
Shape	Round (variable)	Round (variable)	Round (variable)	Round (variable)	Round (variable)
Prolif	Yes	Yes	Limited to none	Yes	Yes
Morph	Two-dimensional monolayer	Three-dimensional multilayers; limited matrix penetration	Rapid aggregate formation; canalicular-like processes	Three-dimensional multilayers; limited matrix penetration	Three-dimensional multilayers; acini formation; limited matrix penetration
Smooth muscle-like cells					
Shape	Spindle, nucleus prominent	Spindle, nucleus prominent	Round	Spindle; nucleus prominent	Spindle; nucleus prominent
Prolif	Yes	Yes	Little to none	Yes	Yes
Morph	Monolayer with aggregated ridges	Monolayer with aggregated ridges; limited matrix penetration	Rapid aggregate formation	Three-dimensional multilayered arrays; matrix penetration	Three-dimensional multilayered arrays; matrix penetration

the substrate surface as a single layer of flattened cells. In contrast, SIS-derived gel induced regional piling of cells into multilayered aggregates. Cells reached confluence between days 7 and 11 on plastic, Vitrogen, and SIS-derived gel. However, even at confluence, cells on plastic maintained a two-dimensional growth pattern (Fig. 8A). While some evidence of multilayer cell aggregation was noted on Vitrogen (Fig. 8B), the most extensive three-dimensional pattern was developed by cells on SIS-derived gel (Fig. 8D). When grown on Matrigel, Clemons cells attached and formed aggregates within 24 h (Fig. 8C). In some cases, the aggregates were connected by long canalicular-like processes. At later time points, the interconnecting structures receded, leaving dense aggregates scattered along the surface. On Matrigel, no significant increase in cell number was noted at any time point up to 14 days. Unlike Matrigel, intact SIS induced attachment, proliferation, and polarization of Clemons cells *in vitro*. Initially, cells grew as aggregates one

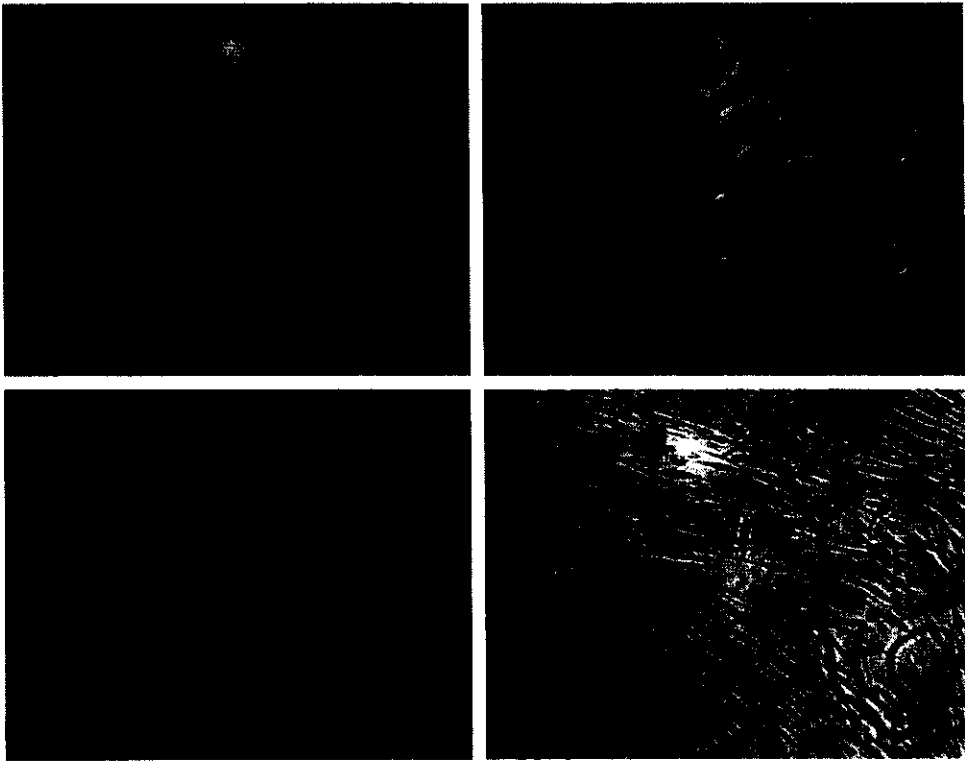


FIG. 4. Morphology ($\times 10$) of mouse fibroblasts on plastic, day 1 (A); Vitrogen day 4 (B); Matrigel, day 1 (C); and SIS-derived gel, day 4 (D).

to three cells thick along the surface of the SIS. By day 7, confluent layer of cells covered the surface of SIS, with some organized areas resembling early follicle formation. By day 14, numerous structures composed of epithelial cells organized around a central lumen were evident, reminiscent of acini (Fig. 9). Although these cells grew primarily along the surface of SIS, in some sections, isolated foci of cells were identified within the matrix (data not shown).

Smooth Muscle-Like Cells

Primary cultures of stromal cells were derived from human urinary bladders and subsequently propagated *in vitro*. Immunohistochemical staining confirmed the presence of vimentin, smooth muscle α -actin, and smooth muscle myosin, characteristic of the smooth muscle phenotype. When grown on plastic, stromal

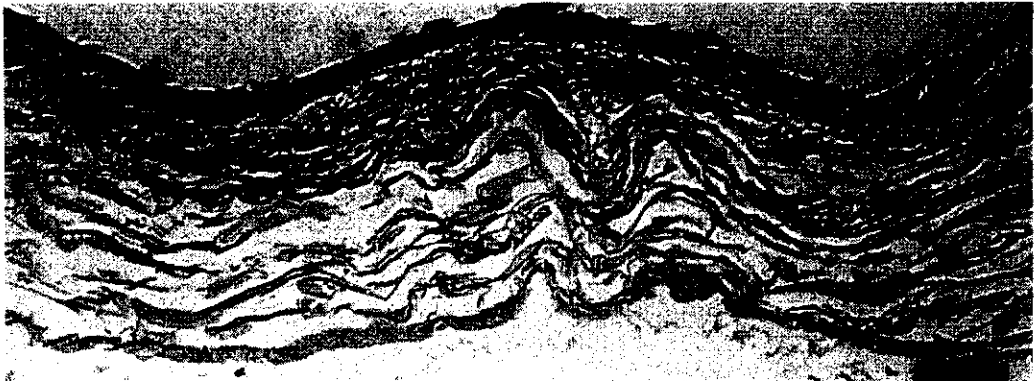


FIG. 5. Light micrograph of H&E-stained cross-section of mouse fibroblasts on intact SIS; day 14. Bar = 50 μm .

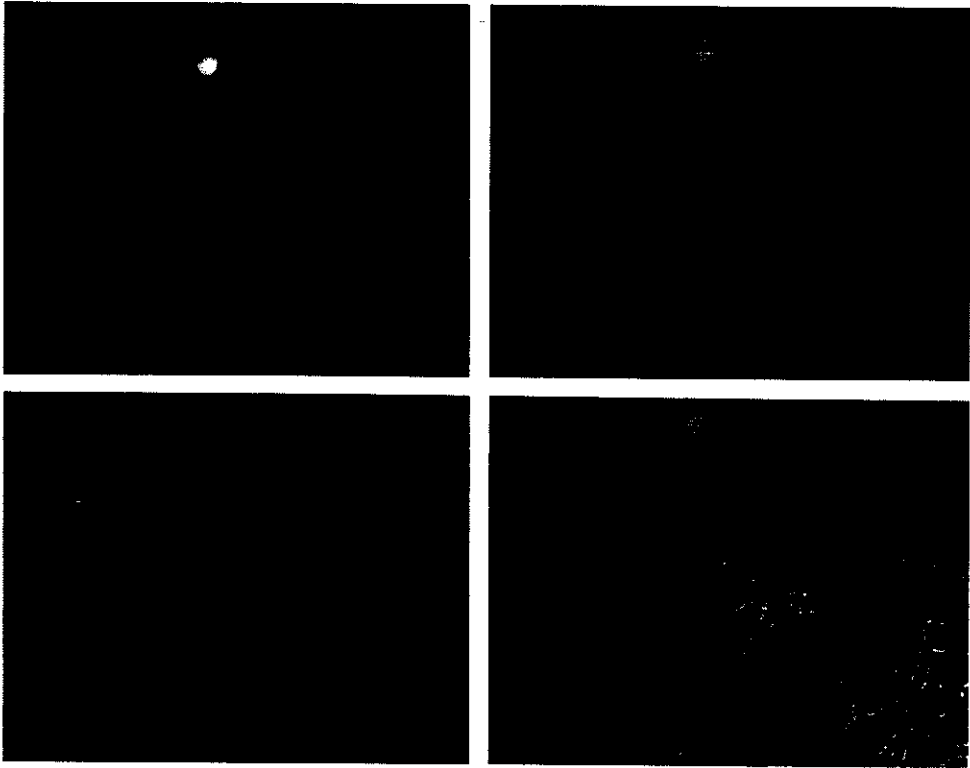


FIG. 6. Morphology ($\times 10$) of rat pulmonary endothelial cells (day 1) on plastic (A); Vitrogen (B); Matrigel (C); and SIS-derived gel (D).

cells displayed a characteristic spindle-shaped morphology, with a centrally located, round to oval nucleus (Fig. 10A). At early time points, up to 4 days, this morphology was observed of stromal cells on Vitrogen and SIS-derived gel. However, as the cells continued to proliferate on the different substrata, distinct morphologies developed. Stromal cells formed aggregated ridges of cells that were grossly and microscopically visible on plastic (Fig. 10A) and Vitrogen (Fig. 10B) as early as 4 days and 7 days, respectively. In contrast, stromal cells grown on SIS-derived gel readily proliferated and penetrated into the matrix to form multiple layers of aligned cells (Fig. 10D). No ridge formation was observed on the SIS substrata at any time point investigated. Matrigel induced a significantly different response characterized by regional aggregates of cells (Fig. 10C). This morphology was observed within the first 24 h of incubation and persisted with no obvious proliferative activity by the cells up to 14 days. The ability of SIS to induce tissue-specific histogenesis was also observed with stromal cells. On SIS, the stromal cells maintained their spindle shape with a centrally located, prominent nucleus. Within 7 days, the cells proliferated and migrated throughout the matrix, organizing into thick bands or multilayers of parallel aligned cells (Fig. 11).

DISCUSSION

Much of our knowledge of form and function at the cell, tissue, and organ levels has come from the isolation of mammalian cells and their culture *in vitro*. In turn, these principles have been applied to develop interdisciplinary strategies for construction of tissue analogues that improve, maintain, or restore tissue structure and function (tissue engineering).²² To date, the majority of cell culture experimentation has been performed in a two-dimensional format on artificial (synthetic) substrata consisting of glass or plastic. Although polystyrene is by far the most commonly used artificial substrate, cells have also been successfully

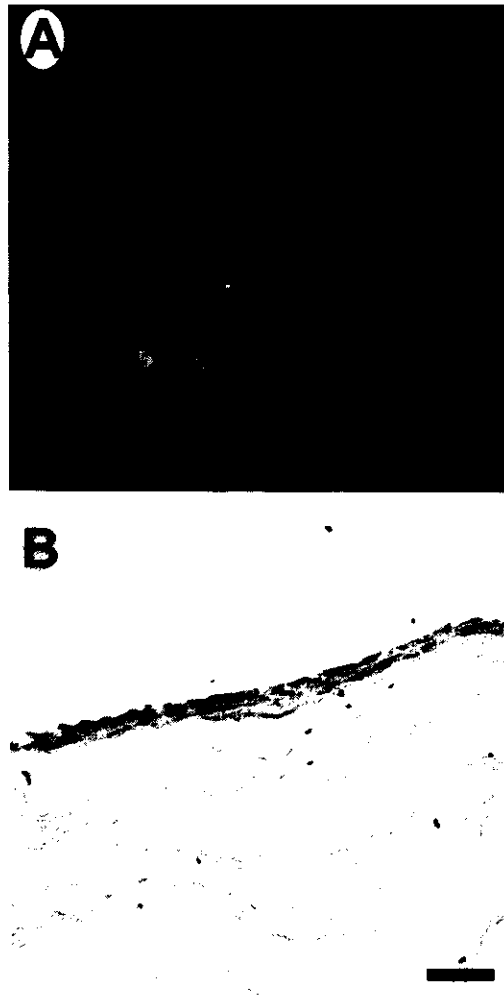


FIG. 7. Fluorescence micrograph of PKH-26-labeled endothelial cells on intact SIS, day 1 (A). Light micrograph of H&E-stained cross-section of rat pulmonary endothelial cells on intact SIS, day 7 (B). Bar = 50 μm .

grown on polyvinylchloride (PVC), polycarbonate, polytetrafluorethylene (PTFE), melinex, and thermanox (TPX).²³ Because of their attractiveness for tissue engineering applications, a number of bioabsorbable synthetic polymers have been investigated for the culture and delivery of cells.²⁴ These include polyglycolic acid, poly L-lactic acid, and polyglycolic-co-lactic acid. Although the chemical and physical properties of these substrata can be controlled, these materials lack the ability of ECM to predictably signal (orchestrate) fundamental cellular processes. Therefore, when cells are isolated from their natural ECM, cultured, and propagated under these conditions, the resultant cell phenotype is often different from that observed in the tissue from which it was derived.

In contrast, SIS represents the ECM of normal porcine intestine in its native composition and architecture. When implanted *in vivo*, SIS induces cellular responses that recapitulate embryogenesis and tissue regeneration in that appropriate tissue structure and function are restored with minimal scar formation.^{11–16} We postulated that maintaining the complex composition and architecture of SIS would enable cells to maintain their *in vivo* phenotype and three-dimensional organization even when cultured *in vitro*. The present study is the first demonstration that different cell types will survive, and develop tissue-like morphology when grown on SIS *in vitro*. Clearly, the architectural and “instructive” properties of SIS are distinct from those of traditional cell culture substrata: plastic, Vitrogen, and Matrigel.

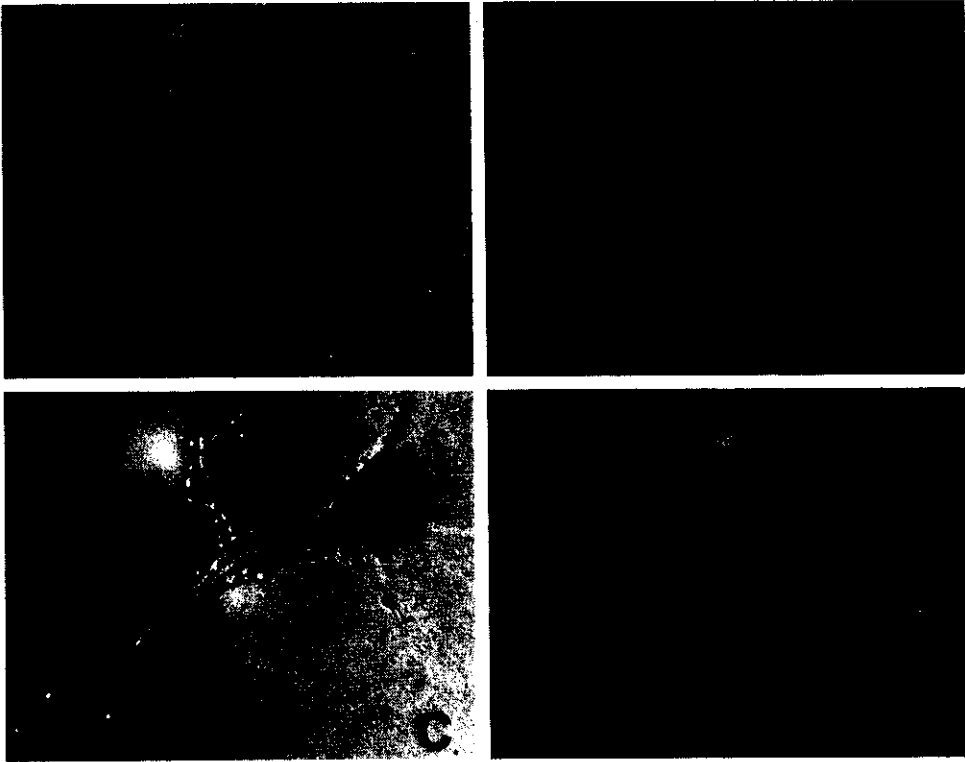


FIG. 8. Morphology ($\times 10$) of canine prostate adenocarcinoma cells on plastic, day 14 (A); Vitrogen, day 14 (B); Matrigel, day 1 (C); and SIS-derived gel, day 14 (D).

As observed with the majority of vertebrate cells, fibroblastic (Swiss mouse 3T3), endothelial (rat pulmonary artery), glandular epithelial (canine prostate adenocarcinoma), and smooth muscle-like (human bladder stromal) cells used in this study were limited to simple two-dimensional morphological patterns when grown on plastic. It is said that continuous exposure of cells to plastic often results in loss of morphology as well as biochemical and functional properties, a process referred to as dedifferentiation.^{25,26} The fact that many molecules of the extracellular matrix exhibit the ability to self-assemble into highly ordered arrays has allowed the development of two routinely used three-dimensional substrata, Matrigel and Vitrogen. Vitrogen represents a more simplified substrate in that it is composed of Type I collagen purified from bovine dermis. Type I collagen was the first macromolecule to be shown to undergo spontaneous assembly *in vitro*.²⁷ Structurally, Vitrogen represents an irregular arrangement of dense fibrillar aggregates laced with a network of thin fibrils. Matrigel, on the other hand, is an extract of basement membrane secreted by Engelbreth Holm Swarm tumor cells *in vitro*, the physiologic relevance of which is uncertain.²⁸ Consisting of collagen IV, laminin, and heparan sulfate proteoglycan along with several growth factors,^{29,30} Matrigel forms a honeycomb structure along the interwoven fibrils of type IV collagen.

We have taken an alternative approach for development of a more physiologically relevant, three-dimensional cell culture substrate. This involves processing of the extracellular matrix derived from the small intestine such that viable cells are eliminated but the natural architecture and composition of the ECM are minimally perturbed. This approach is based upon the principle that polymeric assemblies of ECM are in many cases secreted by cells as precursor molecules that are significantly modified (proteolytically processed, sulfated, oxidized, and cross-linked) before assembly with other components into functional polymers. One consequence of the contribution of this cell processing is that polymers reconstituted in the laboratory with components extracted from extracellular matrices do not have all the properties they have when they are assembled by cells *in vivo*.³¹ SIS, like other naturally occurring ECM, consists predominantly of fibrillar collagens (type I, III, V; unpublished data), proteoglycans, glycosaminoglycans (e.g., hyaluronic

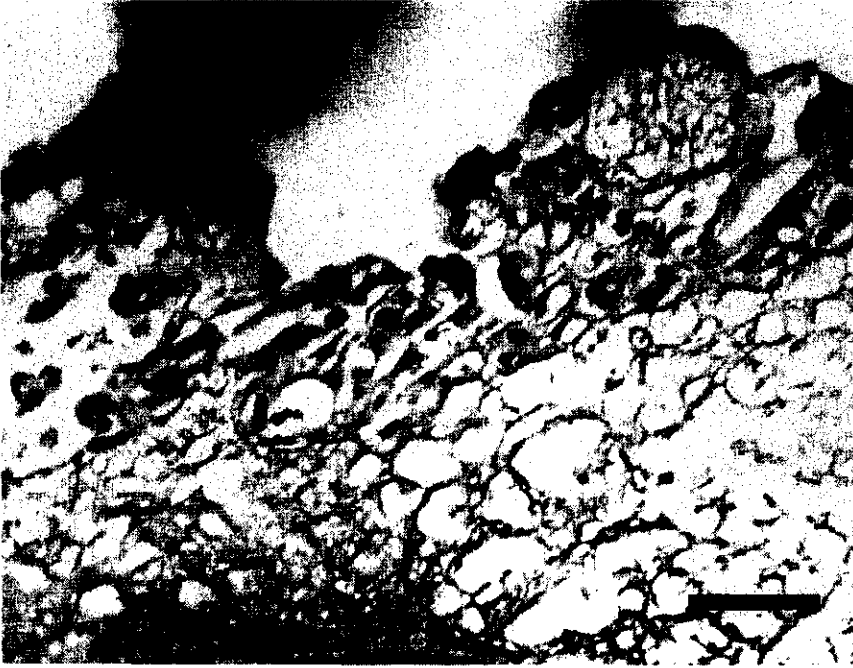


FIG. 9. Light micrograph of H&E-stained cross-section of canine prostate adenocarcinoma cells on intact SIS, day 14. Bar = 50 μm .

acid),¹⁷ glycoproteins (e.g., fibronectin),¹⁸ and growth factors (e.g., FGF-2 and TGF β -related protein).¹⁹ The presence of growth factors in the SIS substrate, likely in association with regulatory binding components (e.g., FGF-2 and heparan sulfate proteoglycan), is expected to influence cell behavior on this substrate.

More recently, we have developed an extract of SIS that can be induced to form a semisolid gel *in vitro*. Unlike SIS in its native form with its definite sidedness, the gelled substrate is nearly homogeneous in architecture. Unlike Matrigel, SIS-derived gel represents an extract of normal tissue created naturally by cells *in vivo*. Preliminary biochemical analysis of SIS-derived gel has revealed it contains multiple components, including at least three collagen types, glycosaminoglycans, and growth factors (unpublished data). Comparison of the architectural features of SIS-derived gel with that of intact SIS further demonstrated that *in vitro* assemblies of less complex mixtures of ECM components lack the sophisticated architecture of extracellular matrices assembled *in vivo*.

The ability of SIS and SIS-derived gel to serve as cell culture scaffolds was demonstrated by the ability of all four cell types studied to attach, survive, proliferate, and, in some cases, differentiate on these matrices. Interestingly, each cell type was distinct in its behavior and appearance when cultured on SIS and SIS-derived gel. Moreover, the importance of substrate architecture and composition on cell behavior *in vitro* was apparent by the disparity in morphologic patterns developed by each cell type on the three-dimensional substrata evaluated. For instance, long-term culture (up to 14 days) of RPEC or Clemons on Vitrogen, SIS-derived gel, and SIS resulted in relatively similar morphologies. On the other hand, patterns developed by 3T3 fibroblasts and bladder stromal cells on SIS and SIS-derived gel were distinct from those observed on the other substrata evaluated. All four cell types responded in a dramatically different fashion when cultured on Matrigel. Matrigel promoted rapid cell-cell interaction with formation of aggregates within 24 h of seeding. This rapid aggregation was accompanied by a loss of proliferative activity, a response documented previously for a number of other cell types, including rat capillary endothelial cells,³² bovine retinal pigmented epithelial and lens cells,³³ mouse Leydig cells,³⁴ and normal and tumor-derived primary human mammary epithelial cells.³⁵

We found that 3T3 fibroblasts attached and proliferated but showed no penetration into the type I col-

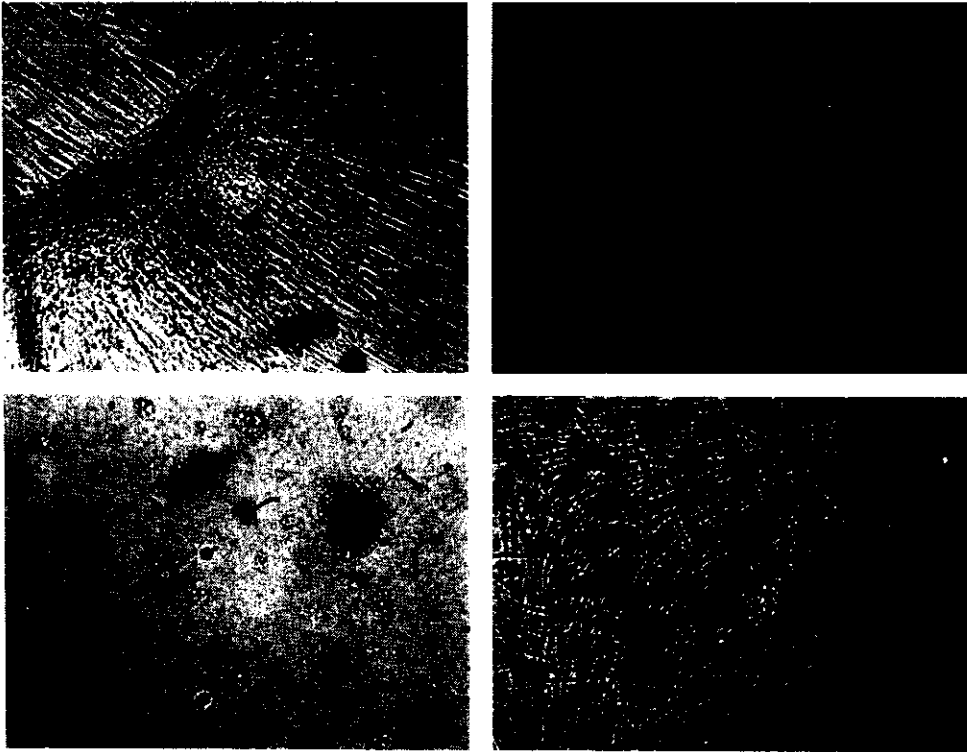


FIG. 10. Morphology ($\times 10$) of stromal cells (day 7) on plastic (A); Vitrogen (B); Matrigel (C); and SIS-derived gel (D).

lagenous network of Vitrogen. In addition, Vitrogen induced formation of a monolayer of cuboidal shaped cells, a pattern similar to that developed by fibroblasts on plastic. These findings are in agreement with studies performed by Elsdale and Bard³⁶ involving human fibroblasts and type I collagen derived from rat tail tendon. In contrast, intact and gelled forms of SIS fostered more cell–substrate interaction as evidence by the fusiform shape and intimate integration of fibroblasts within matrix components. Such behavior and histogenesis is commonplace for the fibroblast phenotype as it occurs naturally in connective tissue structures *in vivo*. In fact, it would be difficult to distinguish the histology generated by fibroblasts cultured on intact SIS *in vitro* from that of a naturally occurring connective tissues such as the dermis or submucosa layer of the intestine.

Previous investigations have shown that the composition of the extracellular matrix plays a significant role in influencing the behavior of endothelial cells *in vitro*.^{32,37,38} Endothelial cells are well known for their ability to form “cobblestone” morphology on plastic. However, in three-dimensional culture, a variety of responses have been observed depending upon cell source (e.g., macrovascular or microvascular) and the nature of the substrata. In the present study, macrovascular RPEC cells formed a layer one to three cells thick across the surface of Vitrogen, SIS-derived gel, and intact SIS. Although some penetration of these matrices was suspected, the majority of cells remained along the surface of the substrata. There have been reports of tube formation as it relates to angiogenesis by endothelial cells in three-dimensional culture.^{39–41} We observed no evidence of such a response by RPEC on either Vitrogen, SIS-derived gel, or intact SIS. The morphological characteristics of RPEC cells to Matrigel observed in the present study are similar to those obtained with rat aorta and human umbilical vein endothelial cells—a response termed “morphological differentiation” by Kubota et al.^{38,42,43} However, further investigations have shown that these morphological changes likely did not involve the typical transcriptional and translation events of endothelial cell differentiation.⁴⁴

The induction of polarization, stratification, and even acini formation by glandular epithelial cells in three-dimensional culture systems is well documented. In fact, tissue-specific phenotypic expression has been ob-



FIG. 11. Fluorescence micrograph of PKH-26-labeled stromal cells on intact SIS, day 7 (A). Light micrograph of H&E-stained cross-section of stromal cells on intact SIS, day 14 (B). Bar = 50 μm .

served with both normal and tumorigenic epithelial cells, including human mammary epithelial cells,^{45,46} rectal adenocarcinoma cells,⁴⁷ and thyroid epithelial cells.⁴⁸ Herein, we demonstrated the ability of canine prostate adenocarcinoma cells to develop three-dimensional morphological patterns when cultured on Vitrogen, Matrigel, SIS-derived gel, and intact SIS but not on plastic. Interestingly, the rapid aggregation on Matrigel stabilized within 24–48 h, with no obvious proliferation. In contrast, both proliferation and differentiation were noted on Vitrogen, SIS-derived gel and intact SIS. The acini formed resembled those that would be expressed by this cell type *in vivo*.

The culture of smooth muscle cells *in vitro* has routinely been difficult due to loss of expression of smooth muscle-specific protein markers (e.g., α -actin, myosin, caldesmon) along with contractile function.⁴⁹ This is the first demonstration of the influence of different ECM substrata on the growth and behavior of human bladder stromal cells. The formation of multilayered arrays without contact inhibition of growth by fetal bovine and human bladder smooth muscle cells on plastic has been reported previously by Baskin.⁵⁰ Although we observed a similar growth pattern with short culture periods on plastic, Vitrogen, SIS-derived gel, and intact SIS, long-term persistence of this pattern (>14 days) occurred only on intact SIS and SIS-derived gel. Stromal cells not only penetrated the matrix but also formed bundles or arrays of parallel aligned cells characteristic of the stromal layer of urogenital tissues from which they were derived.

The ability of SIS to induce tissue-specific morphogenesis of cells was demonstrated initially *in vivo* and now *in vitro*. In summary, for the four cell types investigated, intact SIS and SIS-derived gel were equivalent or superior in their ability to support and maintain expression of tissue-specific phenotype and be-

havior when compared to the routinely used three-dimensional substrata Vitrogen and Matrigel. Future studies will provide a more detailed and quantitative evaluation of how SIS influences adhesion, proliferation, differentiation, and migration of specific cell types. We believe SIS shows promise as a cell culture tool for basic studies of ECM–cell interaction, tissue physiology, metabolism, and morphogenesis as well as for engineering tissue constructs for medical applications.

ACKNOWLEDGMENTS

We are grateful to Deborah Van Horn and Phyllis Lockard of the Electron Microscopy Laboratory of the School of Veterinary Medicine at Purdue University for their technical assistance with electron microscopy and related photography. All SEM was performed at the Electron Microscope Center in Purdue's School of Agriculture under the expert consultation of Debra Sherman. This work was supported by grants from Purdue University Research Foundation (TRASK) and Cook Biotech Inc., West Lafayette, IN.

REFERENCES

1. Bissell, M.J., Hall, H.G., and Parry, G. How does the extracellular matrix direct gene expression? *J. Theor. Biol.* **99**, 31, 1982.
2. Bissell, M.J., and Aggeler, J. Dynamic reciprocity: How do extracellular matrix and hormones direct gene expression? In: Cabot, M.C., and McKeehan, W.L., eds. *Mechanisms of Signal Transduction by Hormones and Growth Factors*. New York: Alan R. Liss, 1987, pp. 251–262.
3. Adams, J.C., and Watt, F.M. Regulation of development and differentiation by the extracellular matrix. *Development* **117**, 1183, 1993.
4. Lelievre, S., Weaver, V.M., and Bissell, M.J. Extracellular matrix signaling from the cellular membrane skeleton to the nuclear skeleton: A model of gene regulation. *Recent Prog. Horm. Res.* **51**, 417, 1996.
5. Leighton, J. Radial histophysiological gradient culture chamber: Rationale and preparation. *In Vitro Cell. Dev. Biol.* **27A**, 786, 1991.
6. Douglas, W.H., McAteer, J.A., Dell'Orco, R.T., and Phelps, D. Visualization of cellular aggregates cultured on a three-dimensional collagen sponge matrix. *In Vitro Cell. Dev. Biol.* **16**, 306, 1980.
7. Dehm, P., and Kefalides, N.A. The collagenous component of lens basement membrane. The isolation and characterization of an alpha chain size collagenous peptide and its relationship to newly synthesized lens components. *J. Biol. Chem.* **253**, 6680, 1978.
8. Rojkind, M., Gatmaitan, Z., Mackensen, S., Giambrone, M.A., Ponce, P., and Reid, L.M. Connective tissue bio-matrix: Its isolation and utilization for long-term cultures of normal rat hepatocytes. *J. Cell Biol.* **87**, 255, 1980.
9. Liotta, L.A., Lee, C.W., and Morakis, D.J. New method for preparing large surfaces of intact human basement membrane for tumor invasion studies. *Cancer Lett.* **11**, 141, 1980.
10. Armstrong, P.B., and Quigley, J.B. Transepithelial invasion and intramesenchymal infiltration of the chick embryo chorioallantois by tumor cell lines. *Cancer Res.* **42**, 1826, 1982.
11. Knapp, P.M., Lingeman, J.E., Siegel, Y.I., Badylak, S.F., and Demeter, R.J. Biocompatibility of small-intestinal submucosa in urinary tract as augmentation cystoplasty graft and injectable suspension. *J. Endourol.* **8**, 125, 1994.
12. Kropp, B.P., Rippy, M.K., Badylak, S.F., Adams, M.C., Keating, M.A., Rink, R.C., and Thor, K.B. Regenerative urinary bladder augmentation using small intestinal submucosa: Urodynamic and histopathological assessment in long-term canine bladder augmentation. *J. Urol.* **155**, 2098, 1996.
13. Prevel, C.D., Eppley, B.L., Summerlin, D.J., Jackson, J.R., McCarty, M., and Badylak, S.F. Small intestinal submucosa (SIS): Utilization for repair of rodent abdominal wall defects. *Ann. Plast. Surg.* **35**, 374, 1995.
14. Badylak, S.F., Tullius, R., Kokini, K., Shelbourne, K.D., Klootwyk, T., Voytik, S.L., Kraine, M.R., and Simmons, C. The use of xenogeneic small intestinal submucosa as a biomaterial for Achille's tendon repair in a dog model. *J. Biomed. Mater. Res.* **29**, 977, 1995.
15. Aiken, S.W., Badylak, S.F., Toombs, J.P., Shelbourne, K.D., Hiles, M.C., Lantz, G.C., and Van Sickle, D. Small intestinal submucosa as an intra-articular ligamentous graft material: A pilot study in dogs. *V.C.O.T.* **7**, 124, 1994.
16. Lantz, G.C., Badylak, S.F., Hiles, M.C., Coffey, A.C., Geddes, L.A., Kokini, K., Sandusky, G.E., and Morff, R.J. Small intestinal submucosa as a vascular graft: A review. *J. Invest. Surg.* **6**, 297, 1993.

17. Hodde, J.P., Badylak, S.F., Brightman, A.O., and Voytik-Harbin, S.L. Glycosaminoglycan content of small intestinal submucosa: A bioscaffold for tissue replacement. *Tissue Eng.* **2**, 209, 1996.
18. McPherson, T., and Badylak, S.F. Characterization of fibronectin derived from porcine small intestinal submucosa. *Tissue Eng.* **4**, 75, 1998.
19. Voytik-Harbin, S.L., Brightman, A.O., Waisner, B., Lamar, C.H., and Badylak, S.F. Identification of extractable growth factors from small intestinal submucosa. *J. Cell. Biochem.* **4**, 478, 1997.
20. Carter, W.O., Narayanan, P.K., and Robinson, J.P. Intracellular hydrogen peroxide and superoxide anion detection in endothelial cells. *J. Leuk. Biol.* **55**, 253, 1994.
21. Singhvi, R., Stephanopoulos, G., and Wang, D. Review: Effects of substratum morphology on cell physiology. *Biotechnol. Bioeng.* **43**, 764, 1994.
22. Martins-Green, M. The dynamics of cell-ECM interactions with implications for tissue engineering. In: Lanza, R.P., Langer, R., and Chick, W.L., eds. *Principles of Tissue Engineering*. Austin: R.G. Landes Company, 1997, pp. 23-46.
23. Freshney, R. *Culture of Animal Cells. A Manual of Basic Technique*. New York: Wiley-Liss, Inc., 1994.
24. Langer, R., Vacanti, J., Vacanti, C., Atala, A., Freed, L., and Vunjak-Novakovic, G. Tissue engineering: Biomedical applications. *Tissue Eng.* **1**, 151, 1995.
25. Horster, M. Tissue culture in nephrology: Potential and limits for the study of renal disease. *Klin. Wochenschr.* **58**, 965, 1980.
26. Lefebvre, V., Peeters-Joris, C., and Vaes, G. Production of collagens, collagenase and collagenase inhibitor during the differentiation of articular chondrocytes by serial subcultures. *Biochem. Biophys. Acta* **1051**, 266, 1990.
27. Gross, J., Hightberger, J., and Schmitt, F. Collagen structures considered as states of aggregation of a kinetic unit. The tropocollagen particle. *Proc. Natl. Acad. Sci. U.S.A.* **40**, 679, 1954.
28. Kleinman, H.K., McGarvey, M.L., Hassell, J.R., and Martin, G.R. Formation of a supramolecular complex is involved in the reconstitution of basement membrane components. *Biochemistry* **22**, 4969, 1983.
29. Kleinman, H.K., McGarvey, M.L., Liotta, L.A., Robey, P.G., Tryggvason, K., and Martin, G.R. Isolation and characterization of type IV procollagen, laminin, and heparan sulfate proteoglycan from the EHS sarcoma. *Biochemistry* **21**, 6188, 1982.
30. Kleinman, H.K., McGarvey, M.L., Hassell, J.R., Star, V.L., Cannon, F.B., Laurie, G.W., and Martin, G.R. Basement membrane complexes with biological activity. *Biochemistry* **25**, 312, 1986.
31. Olsen, B. Matrix molecules and their ligands. In: Lanza, R.P., Langer, R., and Chick, W.L., eds. *Principles of Tissue Engineering*. Austin: R.G. Landes Company, 1997, pp. 47-65.
32. Madri, J.A., and Williams, S.K. Capillary endothelial cell cultures: Phenotypic modulation by matrix components. *J. Cell Biol.* **97**, 153, 1983.
33. Kennedy, A., Frank, R.N., Sotolongo, L.B., Das, A., and Zhang, N.L. Proliferative response and macromolecular synthesis by ocular cells cultured on extracellular matrix materials. *Curr. Eye Res.* **9**, 307, 1990.
34. Vernon, R.B., Lane, T.F., Angello, J.C., and Sage, H. Adhesions, shape, proliferation, and gene expression of mouse Leydig cells are influenced by extracellular matrix in vitro. *Biol. Reprod.* **44**, 157, 1991.
35. Bergstraesser, L.M., and Weitzman, S.A. Culture of normal and malignant primary human mammary epithelial cells in a physiological manner simulates in vivo growth patterns and allows discrimination of cell type. *Cancer Res.* **53**, 2644, 1993.
36. Elsdale, T., and Bard, J. Collagen substrata for studies on cell behavior. *J. Cell Biol.* **54**, 626, 1972.
37. McGuire, P.G., and Orkin, R.W. Isolation of rat aortic endothelial cells by primary explant techniques and their phenotypic modulation by defined substrata. *Lab. Invest.* **57**, 94, 1987.
38. Kubota, Y., Kleinman, H.K., Martin, G.R., and Lawley, T.J. Role of laminin and basement membrane in the morphological differentiation of human endothelial cells into capillary-like structures. *J. Cell Biol.* **107**, 1589, 1988.
39. Folkman, J., and Haudenschild, C. Angiogenesis in vitro. *Nature* **288**, 551, 1980.
40. Maciag, T., Kadish, J., Wilkins, L., Stemerman, M.B., and Weinstein, R. Organizational behavior of human umbilical vein endothelial cells. *J. Cell Biol.* **94**, 511, 1982.
41. Montesano, R., Orci, L., and Vassalli, P. In vitro rapid organization of endothelial cells into capillary-like networks is promoted by collagen matrices. *J. Cell Biol.* **97**, 1648, 1983.
42. Vernon, R., Angello, J., Iruela-Arispe, M., Lane, T., and Sage, E. Reorganization of basement membrane matrices by cellular traction promotes the formation of cellular networks in vitro. *Lab. Invest.* **66**, 536, 1992.
43. Grant, D.S., Lelkes, P.I., Fukuda, K., and Kleinman, H.K. Intracellular mechanisms involved in basement membrane induced blood vessel differentiation in vitro. *In Vitro Cell. Dev. Biol.* **27A**, 327, 1991.
44. Zimrin, A.B., Villeponteau, B., and Maciag, T. Models of in vitro angiogenesis: Endothelial cell differentiation on fibrin but not matrigel is transcriptionally dependent. *Biochem. Biophys. Res. Commun.* **213**, 630, 1995.

45. Barcellos-Hoff, M.H., Aggeler, J., Ram, T.G., and Bissell, M.J. Functional differentiation and alveolar morphogenesis of primary mammary cultures on reconstituted basement membrane. *Development* **105**, 223, 1989.
46. Yang, J., Richards, J., Guzman, R., Imagawa, W., and Nandi, S. Sustained growth in primary culture of normal mammary epithelial cells embedded in collagen gels. *Proc. Natl. Acad. Sci. U.S.A.* **77**, 2088, 1980.
47. Kirkland, S.C. Polarity and differentiation of human rectal adenocarcinoma cells in suspension and collagen gel cultures. *J. Cell. Sci.* **91**, 615, 1988.
48. Chambard, M., Gabrion, J., and Mauchamp, J. Influence of collagen gel on the orientation of epithelial cell polarity: Follicle formation from isolated thyroid cells and from preformed monolayers. *J. Cell Biol.* **91**, 157, 1981.
49. Birukov, K.G., Frid, M.G., Rogers, J.D., Shirinsky, V.P., Koteliansky, V.E., Campbell, J.H., and Campbell, G.R. Synthesis and expression of smooth muscle phenotype markers in primary culture of rabbit aortic smooth muscle cells: Influence of seeding density and media and relation to cell contractility. *Exp. Cell Res.* **204**, 46, 1993.
50. Baskin, L.S., Howard, P.S., Duckett, J.W., Snyder, H.M., and Macarak, E.J. Bladder smooth muscle cells in culture. I. Identification and characterization. *J. Urol.* **149**, 190, 1993.

Address reprint requests to:
Sherry L. Voytik-Harbin, M.S.E.E., Ph.D.
Purdue University
Hillenbrand Biomedical Engineering Center
Hansen Building, Room B050
West Lafayette, Indiana 47907